Contract No.:

This manuscript has been authored by Battelle Savannah River Alliance (BSRA), LLC under Contract No. 89303321CEM000080 with the U.S. Department of Energy (DOE) Office of Environmental Management (EM).

SHAPE-SELECTIVE PALLADIUM and PALLADIUM-COMPOSITE NANOMATERIALS

Simona E. Hunyadi Murph,[1,2*] Sarah Schyck,[1] and Jessica Bass[1]

[1] *Environmental and Legacy Management Directorate*
Savannah River National Laboratory
Aiken, SC, USA

[2] *Department of Physics and Astronomy*
The University of Georgia
Athens, GA, USA

* Corresponding author: Simona.Murph@srnl.doe.gov;
Telephone: 803-646-6761

Abstract

Multifunctional palladium and palladium composite nanomaterials with tailored shapes and compositions are produced by solution chemistries. This includes (a) palladium nanocubes, (b) palladium nanocubes adorned on iron oxide nanospheres, (c) hollow palladium-silver nanospheres, (d) palladium nanospheres adorned on copper fiber, and (e) palladium nanostars adorned on copper fiber. Palladium nanocubes and palladium cubes adorned on iron oxide nanospheres are prepared through a one-step reduction approach in the presence of a structure directing reagent, namely cetyltrimethylammonium bromide. Palladium-silver nanospheres are created through a simple galvanic replacement reaction by using silver spheres as sacrificial template. Copper fibers are decorated with palladium nanostars and nanospheres in a one-step reduction process. The monometallic and bimetallic nanoparticles can be easily purified and retrieved by centrifugation and/or magnetic separation. A series of analytical tools are employed to elucidate nanomaterials' physico-chemical properties, including scanning electron microscopy, energy dispersive X-ray analysis, and ultraviolet - visible spectroscopy.

Keywords: palladium, composite nanomaterials, shape selective, nanocubes, nanospheres, nanostars.

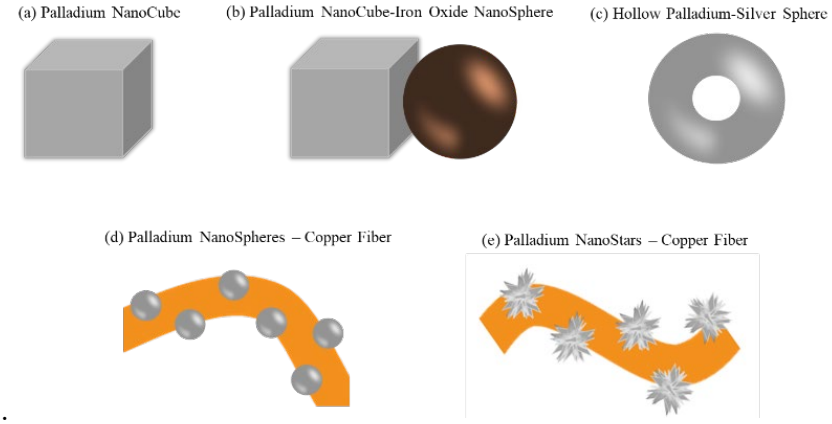

.

1. Introduction

Palladium is one of the most valuable noble metals with extraordinary resistance to oxidation and corrosion [1-3]. It is a soft and ductile metal that can be easily annealed. Its strength and hardness can be, however, significantly amplified at low temperatures [1-3]. These properties make palladium applicable in catalysis [4], electronics [5], dentistry [6], and jewelry [7] sectors. For example, palladium catalysts play a major role as catalytic convertors to reduce pollutant emissions in automobiles [8], in fuel cells arenas [9], and numerous industrial organic reactions [10]. Palladium absorbs large volumetric quantities of hydrogen (around 900 times its volume) at room temperature and atmospheric pressure forming palladium hydride. Additionally, it exhibits rapid sorption kinetics, favorable thermodynamic properties and is high reversibility at low temperature [2, 11, 12]. These unique properties makes it suitable for separation of hydrogen isotopes, separation of hydrogen from gas mixtures, and for hydrogen storage applications [2, 11]. However, limited availability and high cost associated with bulk palladium often hinders its use in industrial processes.

Over the last two decades, development of nanoscale materials received extraordinary attention in the scientific community [2, 3]. This is due to the fact that the nanoscale materials are more active than their bulk counterparts' and provide an enhanced surface-to-volume ratio compared to their bulk components [13, 14]. The available active areas for chemical reactions are crucial in catalytic processes. An increased number of surface atoms often enhance and promote faster kinetics which results in more efficient catalytic reactions. Since most catalytic processes occur at the surface this reduces the amount of material used in chemical reactions [3, 13, 14]. Therefore, the use of nanoscale materials significantly reduces the cost associated with their use in industrial process.

The design and preparation of uniquely shaped nanostructures have been the focus of intense research for decades. At the nanoscale (1 - 100 nm), the electrons are confined in one, two, or three dimensions. Consequently, in this regime, the quantum size effects become dominant [3]. At this scale, the physico-chemical properties depend on nanoparticle's size, shape, surface arrangement and environment [3, 15]. For example, the atoms in the interior of a nanoparticle are highly coordinated, and therefore more stable than those at the nanoparticle's surface. In comparison, atoms on tips or corners of a crystal have more uncoordinated bonds and are more reactive than the edge or in-plane surface atoms [14, 16, 17]. As a result, metallic nanoparticles with sharp edges, sharp corners, or rough surfaces are more active than the spherical counterparts. The nanocatalyst's spatial distribution, surface or catalysts' support composition and electronic structure also influences their catalytic activity and selectivity. Depending on which crystal faces are exposed to the environment, different catalytic activities may be obtainable [14, 16, 17]. For example, higher index planes with a high density of atomic steps and kinks exhibit higher catalytic activities than the low index planes [17].

The selection of nanomaterials with a specific shape is also critical when investigating hydrogen absorption dynamics. A recent study showed that the hydrogen absorption dynamics in individual palladium nanoparticles proceeds through the corners of palladium nanocubes [18]. Moreover, a shape effect on hydrogen-absorption properties of palladium octahedrons and cubes enclosed by {111} and {100} facets, respectively, have been also observed and reported [19]. That

study showed that, while the exposed facets of these two different shapes do not affect their hydrogen-storage capacity, it significantly affects the absorption speed. Specifically, the octahedral palladium nanocrystals display a faster absorption response than the cubes.

Despite the interest in using shape-selective nanomaterials with different crystallographic facets for industrial processes, their routine usage is still restricted. This is due to complications associated with the reproducible preparation of well defined, reliable and stable nanocrystals. The incorporation of these unique nanocrystals in industrial processes relies on one's ability to develop manufacturing processes that are robust, reliable, and cost effective leading to the production of nanomaterials at scale.

This research describes a number of simple solution chemistry approaches for preparation of (a) palladium nanocubes, (b) palladium nanocubes adorned on iron oxide nanospheres, (c) hollow palladium-silver nanospheres, (d) palladium nanospheres adorned on copper fibers, and (e) palladium nanostars adorned on copper fibers. These nanostructures are characterized by a series of analytical tools to elucidate their physico-chemical properties.

2. Experimental Details

2.1. Materials and Instrumentation

Cetyltrimethylammonium bromide (CTAB), iron (III) oxide, sodium tetrachloropalladate, sodium borohydride ($NaBH_4$), and sodium citrate tribasic dehydrate were purchased from Sigma and were used as received. Ascorbic acid (AA) was purchased from J.T. Baker and was used as received. All reagent solutions were prepared using deionized water. Glassware was cleaned with aqua regia solution (HCl/HNO3, 3:1) and thoroughly rinsed with deionized water before use. The nanomaterials are characterized using a scanning electron microscope (Hitachi SU8320). Energy dispersive X-ray spectroscopy (EDS) was used to determine the material's composition and collect compositional mapping and location of individual elements using an Oxford X Max 150 mm^2 Crystal EDS instrument. A Varian Cary 500 scan UV-Vis-NIR Spectrophotometer was used to monitor nanoparticles' optical properties.

2.2. Experimental Section

2.2.1. Palladium Nanocubes Preparation

Palladium nanocubes were prepared by a solution chemistry approach [3]. To a 5 mL solution of 50 mM cetyltrimethylammonium bromide, 500 µL of de-ionized water was added. The solution was heated to 80 °C with stirring. A 100 µL aliquot of 0.1 M sodium tetrachloropalladate was added to the reaction flask. Subsequently, 160 µL freshly prepared 100 mM ascorbic acid solution was added. When the solution turned dark brown the reaction time was started. The solution was heated with stirring for 2 minutes and then removed from heat and allowed to cool on the bench for an additional 18 minutes. Solution turned dark grey indicating production of palladium nanostructures. The nanoparticles were purified by centrifugation at 6000 rpm for 30 minute and redisperse in water.

2.2.2. Palladium Cubes Decorated on Iron Oxide Nanospheres Preparation

Palladium nanocubes were prepared by a reduction approach in the presence of a support, iron oxide nanomaterial, as described elsewhere [2, 20, 21]. To a 5 mL solution of 50 mM cetyltrimethylammonium bromide, 500 μL of 25 mM iron oxide nanoparticles solution was added. The solution was heated to 90.5 °C with stirring. A 50 μL aliquot of 0.1 M sodium tetrachloropalladate and 50 μL de-ionized water was added. With the addition of the palladium solution, the mixture changed from orange to dark brown. At 91.7 °C (~1 min. after sodium tetrachloropalladate added), 160 μL freshly prepared 100 mM ascorbic acid solution was added. When the solution turned dark brown the reaction time was started. The solution was heated with stirring for 20 minutes and then allowed to cool. A magnet was used to separate the palladium - iron oxide nanoparticles from the supernatant. The supernatant was poured off and washed three times with water and centrifuged at 6000 rpm for 30 min. The palladium iron oxide nanoparticles were washed 5 times with water using a magnet [22].

2.2.3. Hollow Palladium-Silver Nanocomposites Fabrication

The galvanic replacement used to create hollow palladium silver nanostructures by addition of sodium tetrachloropalladate to a silver nanosphere solution. Silver nanosphere were prepared by a method reported previously and used as a sacrificial template for creation of hollow silver-palladium nanospheres. Specifically, into a 25 mL Erlenmeyer flask, 150 microliter of silver nanosphere solution was added dropwise in 6 ml aqueous solution of 0.001M of sodium tetrachloropalladate. Addition of 50uL of 0.1M ascorbic acid to the solution creates uniform nanoparticle surfaces. Nanoparticles were purified by centrifugation.

2.2.4. Palladium Nanospheres and Nanostars Adorned on Copper Fiber

A 28.804 mg piece of copper foam was placed in a solution of 1.79 mM cetyltrimethylammonium bromide and 1.79 mM sodium tetrachloropalladate and allowed to stir at either 85 °C or 60°C. After 5 minutes, 160 μL of 0.1 M ascorbic acid was added. Ascorbic acid concentration varied from 2.78mM to 5.56mM. The reaction proceeded with heat and stirring for 2 minutes and then allowed to cool for 18 minutes on the bench. The copper foam was washed with water 5 times then allowed to dry.

3. Results and Discussions

3.1. Preparation and Characterization of Palladium Nanocubes

Anisotropic and isotropic nanostructures of various compositions can be created by a variety of bottom-up and top-down approaches [3, 13, 14, 16, 23]. The most common bottom-up approaches producing uniquely shape nanostructures are seed-mediated approaches, (co)reduction approaches, template synthesis approaches, or galvanic displacement reactions [24-28]. We

reported earlier the production of shape-selective metallic nanostructures such as nanostars, nanorods, nanospheres, dogbones, nanotubes, nanostars, nanotriangles, cubes, octagons, etc. [3]. Our group can also generate a wide plethora of shape-selective nanostructures of distinct crystallographic configurations, (111), (100), (101), etc., and compositions including monometallic, bimetallic and/or metal oxide materials [3].

While monometallic nanostructures received extraordinary attention in the scientific community due to their size and shape dependent properties, in recent years, the landscape of composite nanomaterials have been receiving increased attention. Composite nanomaterials containing two or more elements or materials with dissimilar properties are of interest as they deliver additional degrees of freedom compared to their monolithic counterparts. It allows production of intricate and complex architectures with well-defined architectural arrangements that open the door to a wide array of applications. For example, surface engineering of a core nanomaterial with a secondary nanomaterial could produce attractive composite nanoarchitectures such as core-shell, alloy-like, patchy, hollow or nano-peapods architectures [3, 13, 14, 25, 26]. For example, we expanded the functionality of gold nanoparticles by coupling with a magnetic iron oxide component and created magnetic hybrid nanocomposite materials [20]. The hybrid nanostructures exhibit both plasmonic and magnetic properties making them useful for photothermal catalytic processes, medical sensing, imaging, or MRI contrast agents [25]. The magnetic properties permit non-contact collection and external manipulation of the material by using magnetic fields. Moreover, some studies showed that composite nanostructures with a non-symmetric architecture, e. g. patchy geometry, are more suitable for detection than the symmetric counterparts. For example, patchy silica-silver nanowires are better sensors in comparison to silver nanowires generating 10^9 enhancement effects versus 10^6 promoting increased detection capabilities for trace level of analytes [26].

It is important to mention that, while we and others successful designed and generated a wide array of uniquely shaped nanostructures, the ability to finely control the size, shape and composition of the final product is not trivial. Fine control of the experimental conditions must be taken into consideration when creating shape selective nanostructures as small changes to the reagents order, ratio between the reductant and precursor, timing, temperature, chemicals, stirring, etc. leads to undesired and widely dispersed (size and shape) nanostructures. To achieve the desired shape, nucleation and crystal growth, experimental parameters must be carefully controlled.

In this study, palladium nanocubes were prepared by a simple one-step reduction approach. The reaction takes place by reduction of palladium ion precursor at elevated temperatures (80ºC) in the presence of a surfactant such as cetyltrimethylammonium bromide. The ratio between the palladium ion precursor, structure directing agent, and reducing agent was precisely tailored to allow production of palladium nanocubes that are uniform in size and shape. Cetyltrimethylammonium bromide has a dual role: as a structure directing agent and capping ligand which provides long term stability of the nanomaterial after purification. A mild reducing agent, such as ascorbic acid, was used to control the nanocubes's growth. A strong reducing agent would generate only spheres. The chemical reaction leading to the production of palladium cubes can be represented as follows (**Figure 1**):

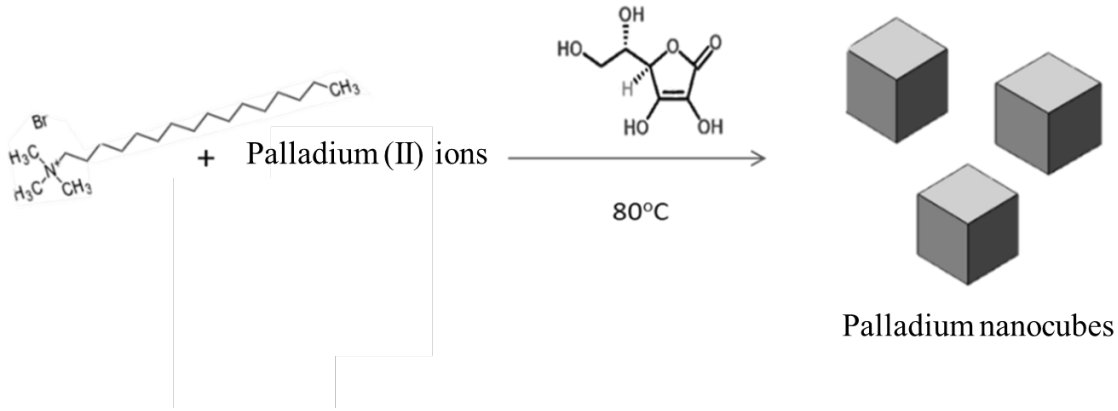

Figure 1. Schematic representation of the chemical reaction leading to the production of palladium nanocubes.

The morphologies of these palladium nanostructures have been investigated using scanning electron microscopy (**Figure 2**). The palladium nanocubes dimension can be tuned by varying the reducing agent concentration and/or by controlling the surfactant concentration. Typically, the length of the cubes can be manipulated from 28nm, 31nm to 34nm. A higher concentration of reducing agent generates nanocubes with larger dimensions. However, it was found that the shape variability also increases with increasing the concentration of the reducing agent. It was also found that the reaction time affects the morphology of the final product. For example, a short reaction time, namely 2 minutes, is most appropriate to create monodisperse in size and shape cubes, i. e. over 90% cubes. A 20-minute reaction time produces cubes, too. However, other shapes, i. e. truncated spherical nanostructures, are generated in the extended reaction time.

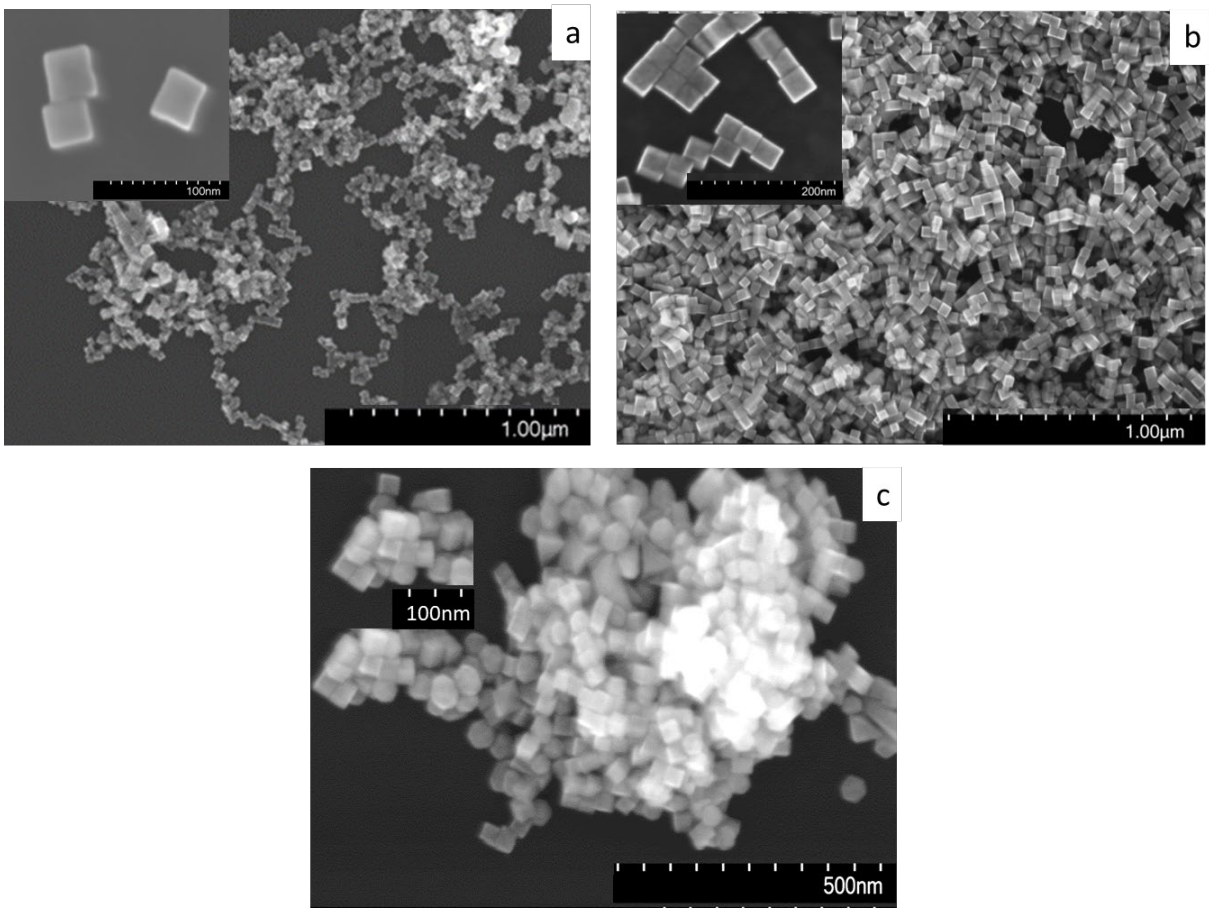

Figure 2. Scanning electron microscopy images of palladium cubes with dimensions (a) 27 nm, (b) 34 nm and (c) 31 nm in length with more variability in shape.

Energy dispersive X-ray analysis (EDS) and mapping was conducted to evaluate the compositional and anatomy of the nanocubes (**Figure 3**). As expected, the data confirm the presence of palladium in agreement with scanning electron microscopy results.

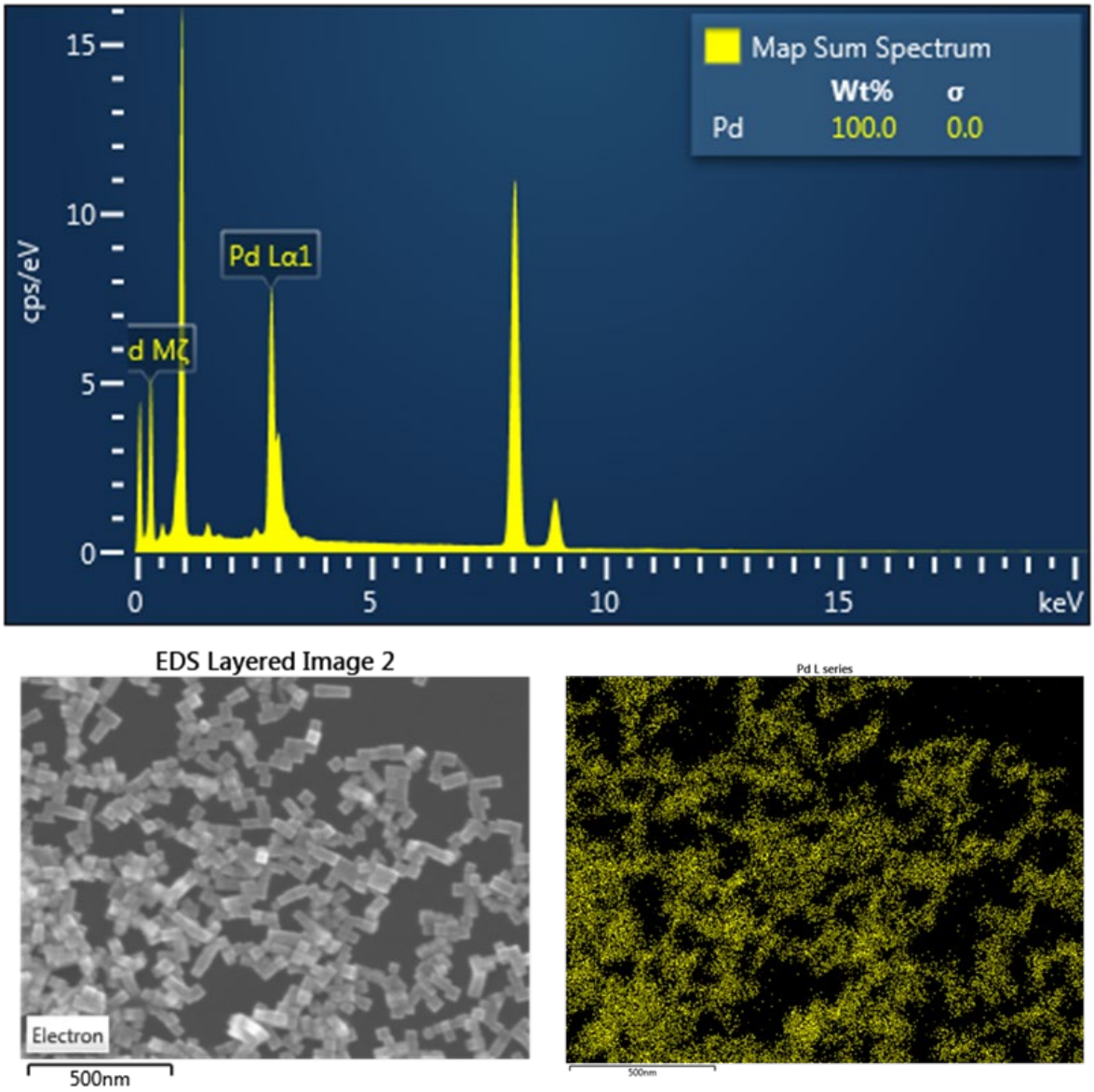

Figure 3. Energy-dispersive spectroscopy data analysis and elemental mapping on palladium cubes.

3.2. Palladium nanocubes adorned on iron oxide nanosphere studies

Development of multifunctional hybrid nanomaterials have received a lot of attention over the years [3, 14, 21, 23]. The hybrid nanomaterials capitalize on their improved properties which are often distinct and cumulative from their constituent individual components. Coupling two or more nanomaterials in various architectures, core-shell, decorated, peapod, hollow structures, generates

composite architectures which influence the crystal structure as well as the electronic and optical properties of the individual materials.

Many industrial processes occur typically at high temperatures requiring materials that are thermally stable. Additionally, regeneration of materials for continued use take place at elevated temperatures. Therefore, the stability and utility of conventional materials is critical in industrial applications. The employment of hybrid structures in which one material serves as an active site for reaction while the secondary one as an 'active/inactive' support are beneficial in high temperature processes [16, 22, 29]. Placing nanocatalysts or nanohydrides on supports could circumvent issues regarding nanomaterial's stability, sintering and durability [2, 30, 31]. The synergistic effects, including short- and long-range interactions, have been documented in literature demonstrating the critical role of the support in a number of industrial processes. Selecting an 'active' support enhances the physico-chemical properties of the material of interest. For example, the support could display magnetic properties that allows manipulation and retrieval by simply using a magnetic field. The distinctive physico-chemical properties of iron-based materials makes them suitable for uses in catalytic reactions, thermal processes, or environmental cleanup activites [2, 20, 21, 32]. We reported earlier the production of multifunctional magnetic-hydride iron oxide-palladium nanomaterials with hydrogen isotope gas storage capabilities [2]. Therefore, hybrid nanomaterials are favorable due to their ability to enhance their functionality . For example, porous iron and hybrid iron-based materials were also successfully used for TcO_4^- sequestration and stabilization from contaminated aqueous media and liquid nuclear wastes [32]. Nanocomposite iron oxide-gold nanoparticles efficiently transduce heat from light and can be magnetically collected and recycled. These properties were exploited in photothermal catalytic reduction of 4-nitrophenol [20, 21].

Palladium ions can be reduced onto iron oxide supports to form nanocubes when using a structure directing reagent, cetyltrimethylammonium bromide, and a mild reducing agent, ascorbic acid. The same procedure used to create palladium cubes have been employed here. At elevated temperature, we decorated iron oxide with palladium nanocubes through a metal ion reduction. Iron oxide nanospheres serve as seed supports. The magnetic properties of iron oxide nanospheres which are in maghemite phase, can be also useful for subsequent recovery and purification with an external magnet. It was found that addition of iron oxide nanoparticles in the reaction vessel affects the final size and morphology on the palladium nanocubes produced (**Figure 4**). Specifically, nanoparticle's dimensions are slightly reduced when the iron oxide seeds are present. The cubes produced in the presence of iron oxide have dimensions of 28nm regardless of the reaction time, 2 minutes or 20 minutes. Additionally, other shapes are being created besides palladium cubes, i. e. spheres, rods, and other undefined truncated nanoparticles.

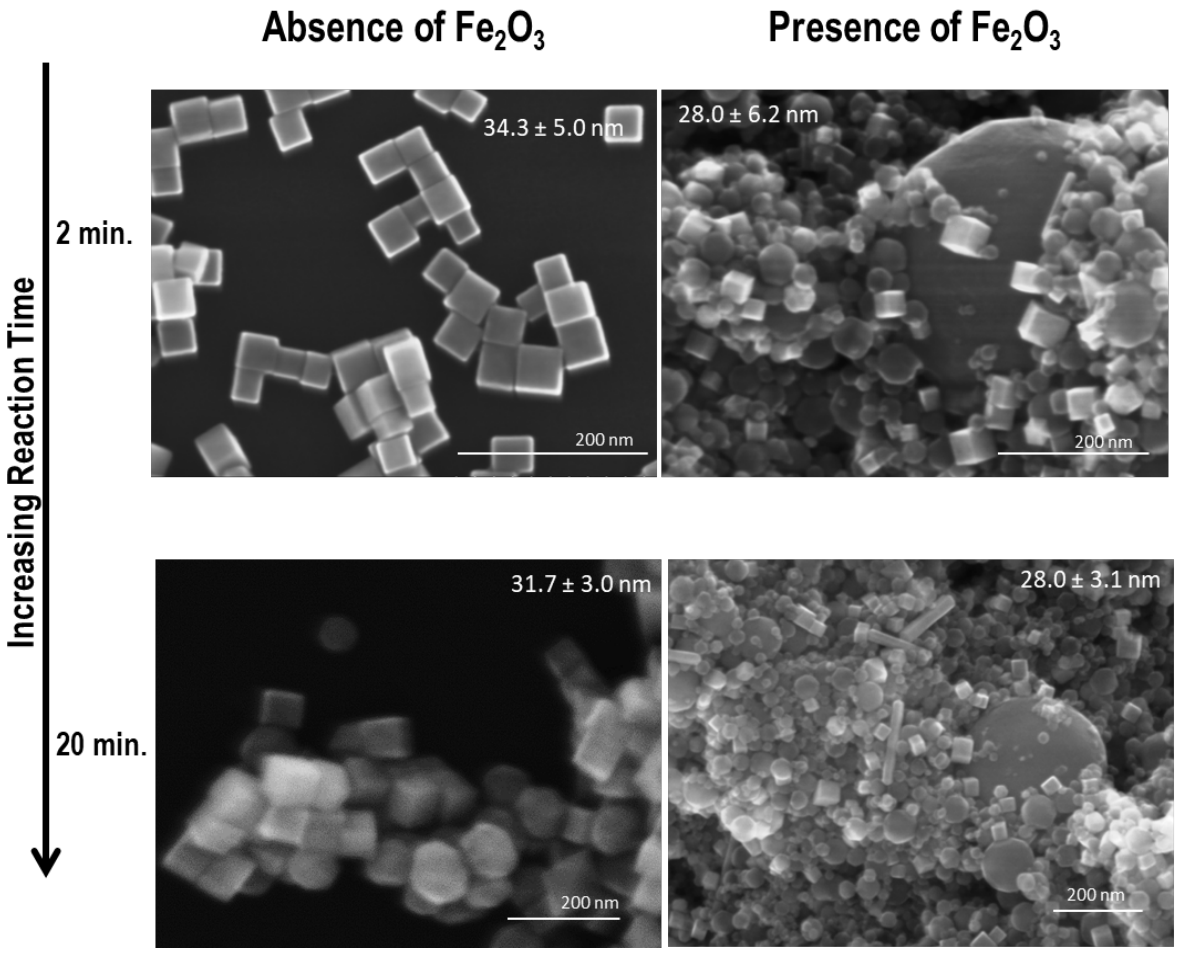

Figure 4. Comparison of control palladium cubes with palladium cubes decorated on iron oxide nanospheres. Less variation of nanocube's morphology and more defined cubes are produced at shorter reaction time (2 minutes vs. 20 minutes). There is more variation in shape of palladium nanocubes and decreased size of nanocubes when iron oxide is added.

The compositions of the different structures have been investigated by energy dispersive X-ray analysis (EDS), line data and mapping examination. These studies confirm production of hybrid material composition, shape and local distribution (**Figure 5**). The mapping analysis shows the distribution and location of main components, palladium and iron, while the line scanning confirms the compositional structure of the materials. Results are in agreement with the scanning electron microscopy results showing that the cubes are palladium while spherical nanostructures are iron. Backscattering images and scanning electron microscopy image clearly show the distribution and location between the dissimilar components namely palladium (electron dense) and iron (less electron dense).

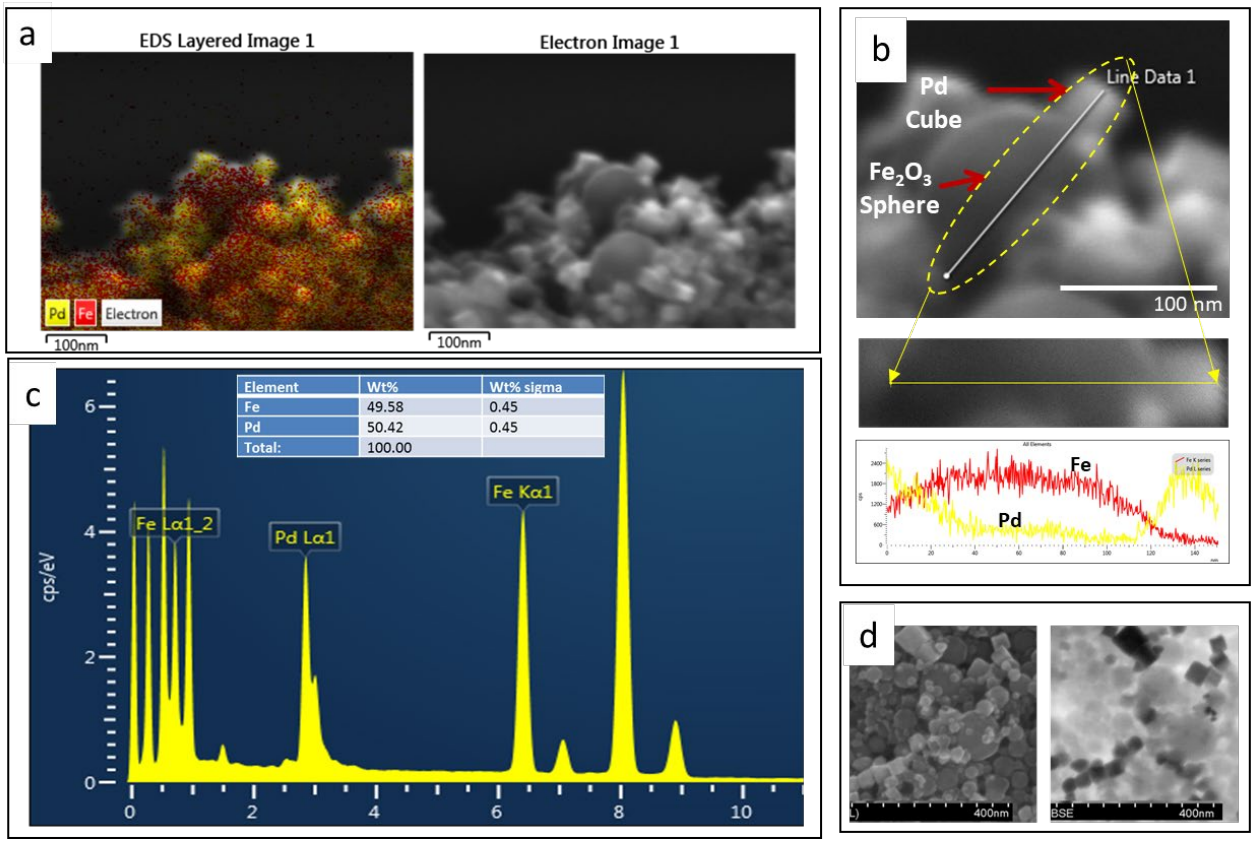

Figure 5. Energy dispersive X-ray analysis, line data and mapping; (a) mapping shows the distribution and location of main components, (b) line scanning confirm the compositional structure of the materials in agreement with the scanning electron microscopy: palladium cube and spheres iron; (c) energy dispersive X-ray analysis identify the elemental peak location and quantitative data of each component; (d) backscattering images and scanning electron microscopy image.

3.3. Hollow palladium-silver nanostructures galvanic displacement studies

Hollow nanomaterials are of long-standing interest since this architecture reduces the materials mass and cost while expanding the reactive surface area [3, 21]. This conformation creates systems that are more efficient as additional surface area is being created. As a result, the concerns regarding the cost associated with the use of noble palladium is often alleviated by using hollow nanomaterials.

Galvanic replacement reactions have been used to good effect here to synthesize hollow palladium-silver nanomaterials starting from silver precursors [27]. In this reaction, silver nanospheres serves as sacrificial template precursors. This reaction is not spontaneous at room temperatures based on each component's reduction potentials. For example, Ag^{+}/Ag^{0} has a standard reduction potential +0.8V, and the analogous potential for $PdCl_4^{2-}/Pd^{0}$ is +0.591V. However, at high temperatures the reaction is spontaneous as $PdCl_4^{2-}$ ions are thermally decomposed at 60ºC into Pd^{2+} and Cl^{-} [33]. Therefore, the reaction at high temperatures proceeds

based on the standard electrode potential of Pd^{2+}/Pd^{0} is +0.951V vs. SHE. The overall reaction that takes place at high temperature is:

$$2Ag^{0} + Pd^{2+} \rightarrow Pd^{0} + 2Ag^{+}$$

The schematic of the galvanic displacement reaction and dealloying/alloying process is described below (**Figure 6**):

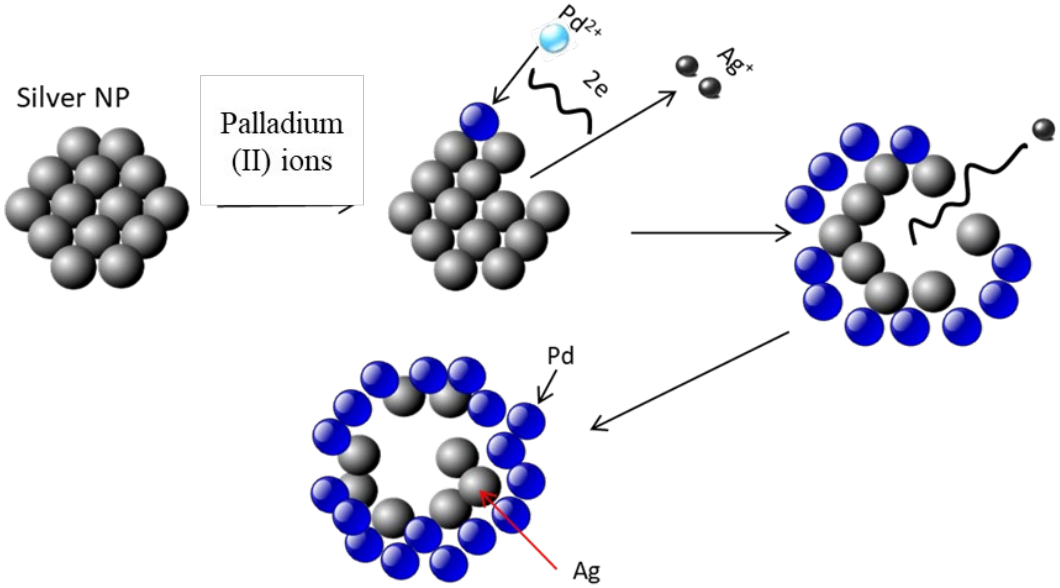

Figure 6. Schematic showing the galvanic displacement reaction and dealloying/alloying process.

The galvanic replacement reaction is initiated on the silver nanosphere surface upon addition of palladium ions. At the beginning, the displacement reaction commences when silver metal is oxidized forming silver ions at the expense of palladium ions. The newly formed silver ions are released in the aqueous solution while palladium ions are being reduced to palladium metal. As the reaction proceeds, the newly formed palladium atoms nucleate on the silver nanosphere in a more or less disordered fashion resulting in an alloy-cluster-type structure. As the reaction continues, more core silver metal is being replaced generating hollow structures. The newly formed hollow structures have a palladium-silver shell. If reaction continues, all silver is replaced leading to hollow palladium spheres. The hollow core dimensions are generally governed by the original diameter of silver nanospheres. The palladium wall thickness and composition can be tailored in dimensions by simply manipulating the palladium ion concentration.

Scanning electron microscopy studies (**Figure 7 a,b**) were conducted to elucidate the nanomaterials dimensions and morphologies. The original silver nanospheres have a diameter of 31±2nm. The hollow palladium-silver nanostructures have a diameter of 52±3nm with a thin shell with dimensions of 11±3nm. The hollow nanostructures have a non-uniform shell with a number of protuberances, valleys and islands indicating that the displacement and alloying process was successful. A smooth shell can be created by additional of a reducing agent which reduces more ions on the nanoparticle's surface. The monometallic and bimetallic structures optical properties

were investigated by ultraviolet-visible spectroscopy (**Figure 7 c, d**). The silver nanospheres have a plasmonic band around 470 nm in agreement with previous studies. At the same time, as expected, the ultraviolet - visible spectra of the bimetallic palladium are slightly different. A blue shift is recorded on the bimetallic nanostructures demonstrating that the bimetallic nanostructure is an alloy structure. X-Ray energy dispersive microanalysis of was performed to investigate the composition of nanostructures before and after galvanic displacement reaction. The elemental map shows clearly that the final bimetallic is composed of both metal and not disparate nano-entities. These studies are in agreement with the spectroscopy data.

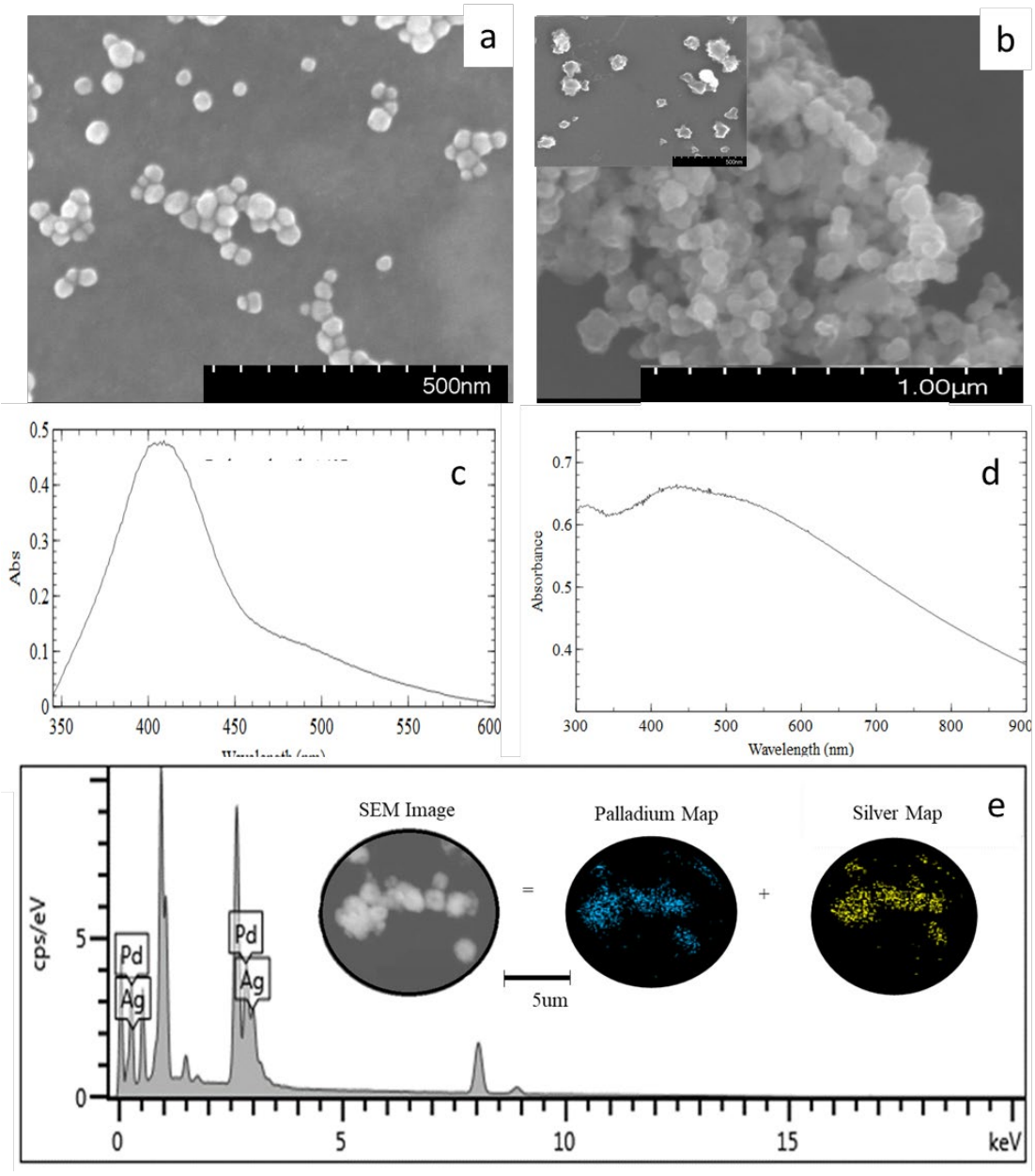

Figure 7. Scanning electron images of (a) silver nanospheres, (b) palladium-silver hollow nanospheres; Ultraviolet - visible spectra of (c) Ag nanospheres, and (d) bimetallic palladium-

silver colloids; (e) X-ray energy dispersive microanalysis of bimetallic palladium-silver hollow nanostructures (inset shows elemental mapping of palladium and silver).

3.4. Palladium Nanospheres and Nanostars Adorned on Copper Fiber

A large number of studies have been developed to create nanoparticles of various shapes and composition in solution [3]. Integration of nanomaterials in various applications, however, require the use of nanoparticles that are bound or directly grown to macro- or nanoscale surfaces. In this study, palladium nanospheres and nanostars were grown onto copper fiber support through a reduction process and/or galvanic displacement reaction (**Figure 8**). Both procedures can be easily scaled up.

X-ray energy dispersive microanalysis before after decoration of copper fibers with palladium nanostructures (**Figure 9**). These results confirm that the copper fibers are effective substrates for treatment with palladium colloids. Elemental mapping shows the formation of palladium colloidal structures on the entire surface of copper fibers. Compositional analysis shows that the fibers contain approximatively 16.5% weight palladium colloids when experiments are conducted at low temperature of 65ºC.

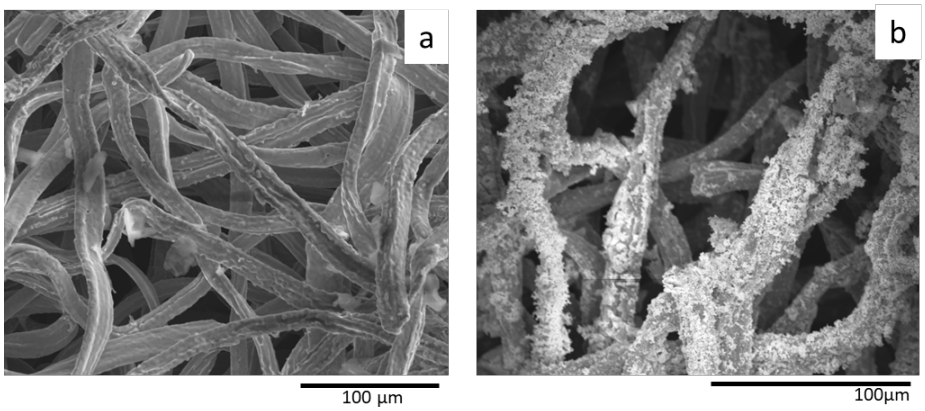

Figure 8. Scanning electron microscopy images of (a) copper fibers support and (b) palladium colloids adorned on copper fibers support (reaction conducted at high temperature).

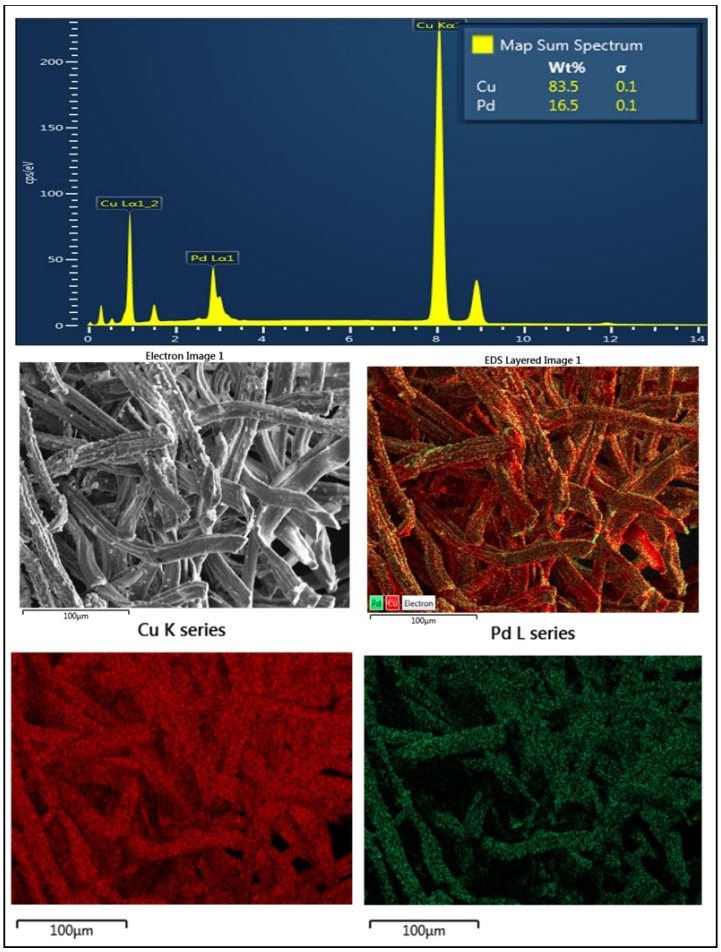

Figure 9. X-ray energy dispersive microanalysis of palladium nanospheres generated on copper fibers at low temperatures: (top) semi-quantitative analysis and (bottom) elemental mapping of palladium and copper.

The size and geometry of the nanoparticles' formation is intimately tied to the experimental conditions used. This includes reaction temperature and presence/absence/amount of reducing agent. For example, a reaction temperature of 85°C generates palladium nanostars with dimensions of 500nm-800nm in diameter while a 60°C generates spherical clusters with dimensions around 500nm (**Figure 10**). An increased in temperature generates more defined nanostars with well-defined spike formations. A higher concentration of reducing agent also results in more defined nanostars. This is not surprising as the reaction continues after an initial nucleation and growth process that produces spherical structures. As more precursor ions are still present in solution the reaction continues. The spikes are being generated on these nanosphere's surface, due to possible various crystal facets, as the palladium ions are slowly reduced by the mild reducing agent through a diffusion and coalescence. The unique spike/rod like structure is also affected and could be attributed to the presence of cetyltrimethylammonium bromide which is a known structure-directing agent. Cetyltrimethylammonium bromide controls the crystallization process by undergoing adsorption-desorption equilibrium that modifies the crystal's surface free energy and stabilize the nanoparticles. It was found that ahigher temperature results in higher concentration of palladium on copper fibers. Specifically, 29.3 wt % palladium is being created at higher

temperature while only 22.6 wt % palladium is produced on the support at lower temperature. It was found that the amount of palladium colloids created on copper fibers can be controlled. For example, according to the X-ray energy dispersive microanalysis, we can tune the amount of palladium on copper fibers from 17, 23, 29 to 33 percent weight. While X-ray energy dispersive microanalysis is a useful qualitative tool to evaluate nanomaterial composition, for a more rigorous metal quantitation additional analytical tools are needed. Inductively coupled plasma atomic emission spectroscopy is being currently explored to completely to quantitate the amount of metals.

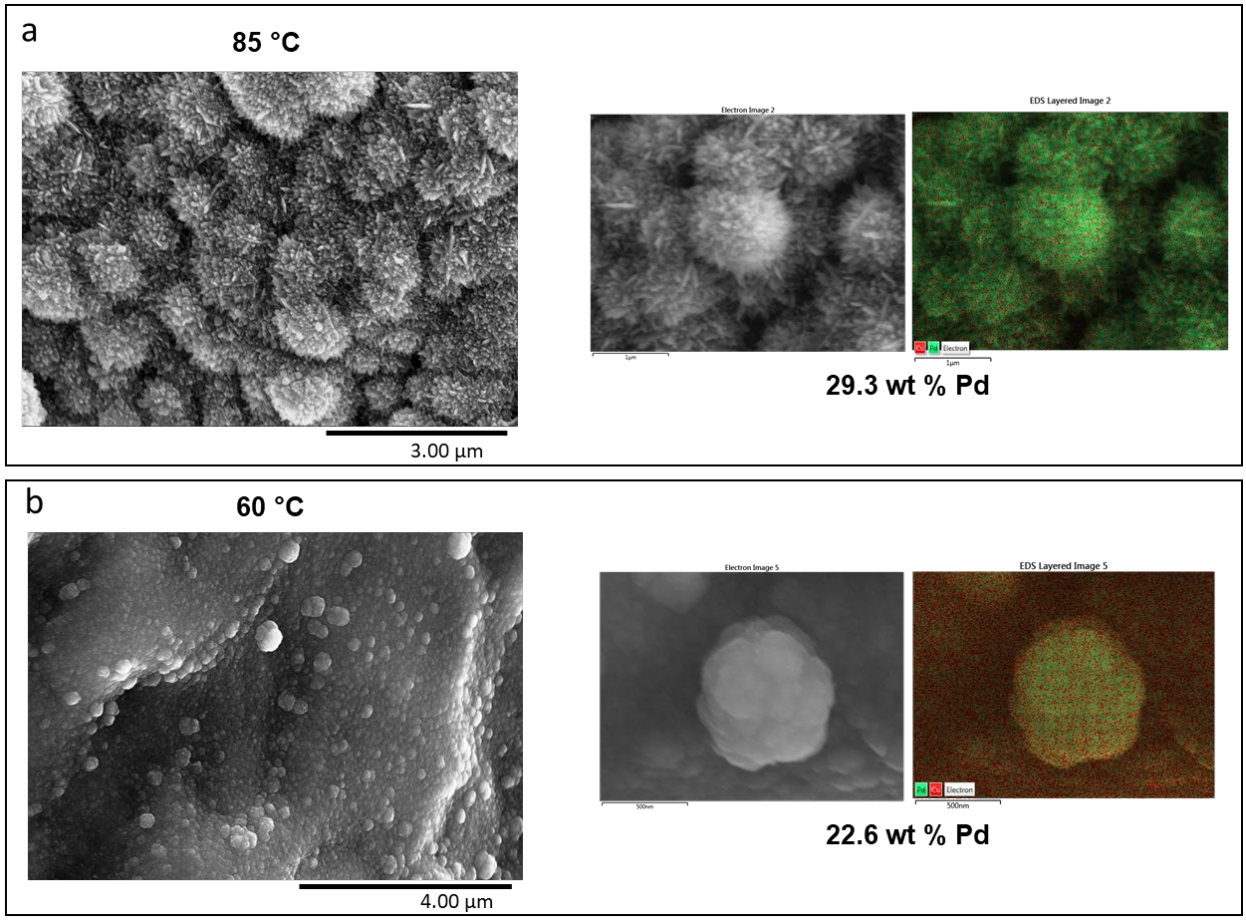

Figure 10. Scanning electron images and accompanying X-ray energy dispersive microanalysis elemental mapping of (a) palladium nanostars adorned on copper fibers, and (b) palladium nanospheres adorned on copper fibers.

4. Conclusions

Multifunctional shape selective palladium and palladium-based nanostructures were synthesized through reduction and/or galvanic displacement methods. Specifically, a library of palladium and composite palladium-based nanomaterials of various sizes, shapes, morphologies and compositions were produced. This includes: (a) palladium nanocubes, (b) palladium

nanocubes adorned on iron oxide nanospheres, (c) hollow palladium-silver nanospheres, (d) palladium nanospheres adorned on copper fiber, and (e) palladium nanosphere adorned on copper fiber. Delicate control of the experimental parameters produces different morphologies and loading on copper fiber supports.

Palladium cubes adorned on iron oxide nanospheres were prepared in one step reduction approach in the presence of a structure directing reagent, namely cetyltrimethylammonium bromide. Decorating palladium nanocubes on iron oxide resulted in similar morphologies to the pure palladium cubes. Palladium-silver hollow composite nanospheres were created through a simple galvanic replacement reaction by using silver spheres as sacrificial templates. The hollow core dimensions are generally governed by the original diameter of silver nanospheres. The palladium wall thickness and composition can be tailored in dimensions by simply manipulating the palladium ions concentration and reducing agents engagement. Copper fibers were also decorated with palladium nanostars and nanospheres in a one-step reduction process.

Reactions are amenable to scale up and can be used in industrial processes. A series of analytical tools were employed to elucidate their physico-chemical properties, including scanning electron microscopy, energy dispersive X-ray analysis, and ultraviolet - visible spectroscopy. The monometallic and bimetallic nanoparticles can be easily purified and retrieved by centrifugation or magnetic separation. The resulting nanocomposite materials retain the physico-chemical properties of the original components. Growth mechanisms that rely on nucleation, growth, oriented attachment, and/or Ostwald ripening effect are proposed. The shape-selective palladium and palladium composite nanostructures described here could be used in catalytic processes, as hydride storage materials, hyperthermia treatment, magnetic resonance imaging contrast agents, among others.

5. Acknowledgments

This work was supported by the Laboratory Directed Research and Development (LDRD) program within the Savannah River National Laboratory (SRNL). This work was produced by Battelle Savannah River Alliance, LLC under Contract No. 89303321CEM000080 with the U.S. Department of Energy. Publisher acknowledges the U.S. Government license to provide public access under the DOE Public Access Plan (http://energy.gov/downloads/doe-public-access-plan).

6. References

1. Griffith, WP; Robinson, SD; Swars, Kurt (2013) Palladium: Palladium Compounds, Springer Publisher.

2. Hunyadi Murph SE, Lawrence K, Sessions H, Brown M, Larsen G (2020) Controlled Release of Hydrogen Isotopes from Hydride-Magnetic Nanomaterials, **ACS Applied Materials & Interfaces**, 12: 9478-9488.

3. Hunyadi Murph SE, Larsen G, Coopersmith K (2017) Anisotropic and shape-selective nanomaterials: structure-property relationships, nanostructure science and technology series. Springer Publisher, pp 1-470.

4. Melián-Cabrera, I (2021) Catalytic Materials: Concepts To Understand the Pathway to Implementation, **Ind. Eng. Chem. Res.,** ASAP.

5. Antler, M. (1982) Fretting of electrical contacts: An investigation of palladium mated to other materials, **Wear**, 81: 159-173.

6. Roy R (2004) Palladium in Restorative Dentistry: Superior Physical Properties make Palladium an Ideal Dental Metal. **Platinum Metals Review** 48: 49–63.

7. Hesse, RW (2007) Palladium. Jewelry-making through history: an encyclopedia. Greenwood Publishing Group. p. 146.

8. Adams, BD, Chen, A (2011) The Role of Palladium in a Hydrogen Economy Mater. **Today,** 14: 282–289.

9. Guo, S, Wang, E. (2011) Noble Metal Nanomaterials: Controllable Synthesis and Application in Fuel Cells and Analytical Sensors **Nano Today**, 6: 240– 264.

10. King, AO, Yasuda, N (2004). Palladium-Catalyzed Cross-Coupling Reactions in the Synthesis of Pharmaceuticals. Organometallics in Process Chemistry. Topics in Organometallic Chemistry. 6. Heidelberg: Springer. pp. 205–245.

11. Rusman, NAA, Dahari, M. (2016) A Review on the Current Progress of Metal Hydrides Material for Solid-State Hydrogen Storage Applications. **Int. J. Hydrog. Energy**, 41: 12108−12126.

12. Jin, Y, Wang, L, Hara, M Watanabe, K (2007) Kinetics of Hydrogen Isotope Absorption for Well-Annealed Palladium-Platinum Alloys. **Mater. Trans.**, 48: 560−565.

13. Hunyadi Murph, SE; Heroux, K, Turick, C, Thomas, D. (2012) Metallic and Hybrid Nanostructures: Fundamentals and Applications, in Applications of Nanomaterials, Series ISBN: 1-62699-000-X, Vol.4: Nanomaterials and Nanostructures, Volume (4), J.N. Govil, ISBN: 1-62699-004-2, Studium Press LLC, USA.

14. Hunyadi Murph, SE, Serkiz, S, Fox, E, Colon-Mercado, H et al (2011) Synthesis, Functionalization, Characterization and Application of Controlled Shape Nanoparticles in Energy Production", Fluorine-Related Nanoscience with Energy Applications, ACS Symposium Series, Volume 1064, Chapter 8, 127-163.

15. Tao, CG, Cullen, WG, Williams, ED, Hunyadi, SE, Murphy, CJ (2007) Surface Morphology and Step Fluctuations on Silver Nanowires, **Surface Science**, 601: 4939- 4943.

16. Hunyadi Murph, S.E. (2020) Shape-Selective Mesoscale Nanoarchitectures: Preparation and Photocatalytic Performance, **Catalysts** 10: 532.

17. Hunyadi Murph SE, Murphy C, Colon-Mercado H, Torres R, Heroux K, Fox E, Thompson L, Haasch R (2011) Tuning of Size and Shape of Au-Pt Nanocatalyst for Direct Methanol Fuel Cells, **J. Nanoparticle** Research,13: 6347-6364.

18. Naraya, T, Hayee, F, Baldi, A, Koh, AL, Sinclair, R, Dionne, JA (2017) Direct visualization of hydrogen absorption dynamics in individual palladium nanoparticles, **Nature Communications,** 8: 14020.

19. Li, G, Kobayashi, H, Dekura, S, Ikeda, R, Kubota, Y, Kato, K, Takata, M, Yamamoto, T, Matsumura, S, Kitagawa, H (2014) Shape-Dependent Hydrogen-Storage Properties in Pd Nanocrystals: Which Does Hydrogen Prefer, Octahedron (111) or Cube (100)? **J. Am. Chem. Soc.** 136: 10222–10225.

20. Larsen, G; Farr, W; Hunyadi Murph, SE (2016) Multifunctional Fe2O3-Au Nanoparticles with Different Shapes: Enhanced Catalysis, Photothermal Effects, and Magnetic Recyclability, **J. Phys. Chem. C**, 120: 15162- 15172.

21. Hunyadi Murph, SE; Larsen, G; Lascola, R (2016) Multifunctional Hybrid Fe2O3-Au Nanoparticles for Efficient Plasmonic Heating, **J. Visual Experiments (JOVE)**, 108: e53598, doi:10.3791/53598.

22. Hunyadi Murph SE, Searles, E (2021) Iron Oxide-Gold Composite Nanoparticles and Nano-Gap Junctions for Sensing Applications Using Surface -Enhanced Raman Scattering, in T.S. Srivatsan, W. Harrigan, Hunyadi Murph, S.E. Metal-Matrix Composites: Advances in Analysis, Measurement, and Observations, Springer Publisher, pp. 93-110.

23. Srivatsan, TS, Harrigan, W, Hunyadi Murph, SE (2021) Metal-Matrix Composites: Advances in Analysis, Measurement, and Observations, Springer Publisher, pp. 93-110.

24. Hunyadi Murph, S.E.; Coopersmith, K. (2020) Fabrication of Silver–Rhodium Nanomaterials for Chemical Sensing Applications. In: Srivatsan T., Gupta M. (eds) Nanocomposites VI: Nanoscience and Nanotechnology in Advanced Composites. The Minerals, Metals & Materials Series. Springer, Cham, 95-104.

25. Hunyadi Murph SE, Jacobs S, Siegfried M, Hu T, Serkiz S, Hudson J (2012) Manganese-Doped Gold Nanoparticles as Positive Contrast Agents for Magnetic Resonance Imaging (MRI), **J. Nanoparticle Res.**, 14: 658-659.

26. Hunyadi Murph, SE; Murphy, CJ (2013) Patchy Silica-Coated Silver Nanowires as SERS Substrates, **J. Nanoparticle Res.**, 15: 1607.

27. Hunyadi, SE; Murphy, CJ (2009) Synthesis and Characterization of Silver-Platinum Bimetallic Nanowires and Platinum Nanotubes, **Journal of Cluster Science**, 20: 319-330.

28. Murphy, CJ, Sau, TK, Gole, AM, Orendorff, CJ, Gao, J, Gou, L, Hunyadi, SE, Li, T (2005) Anisotropic Metal Nanoparticles: Synthesis, Assembly, and Optical Applications, **J. Phys. Chem. B**, 109: 13857-13870.

29. Hunyadi Murph, SE, Goriounova, AA (2020) Study Aimed at Understanding the Use of Nanomaterial-Treated Filters for the Uptake of Heavy Metals from Water Sources, Metal-Matrix Composites: Advances in Analysis, Measurement and Observations, Springer.

30. Hunyadi, SE, Murphy, CJ (2006) Tunable One-Dimensional Silver-Silica Nanopeapod Architectures, **J. Phys. Chem. B**, 110: 7226-7231.

31. Hunyadi Murph, SE, Larsen, GK, Korinko, P, Coopersmith, KJ, Summer, AJ, Lewis, R (2017) Nanoparticle Treated Stainless Steel Filters for Metal Vapor Sequestration, **JOM**, 69: 162-172.

32. Li D, Seaman J, Hunyadi Murph SE, Kaplan D, Taylor-Pashow T (2019) Porous iron material for TcO_4^- and ReO_4^- sequestration from groundwater under ambient oxic conditions. **Journal of Hazardous Materials**, 374: 177-185.

33. Wu, KJ, Gao, Y, Torrente-Murciano, L (2018) Designing Nanoparticle Systems for Catalysis, Continuous synthesis of hollow silver–palladium nanoparticles for catalytic applications, **Faraday Discussions**, 208: 427-441.